CDF Note 11157

Measurement of WW and WZ production in the lepton+Heavy Flavor jets channel in the full CDFII dataset

The CDF Collaboration
URL http://www-cdf.fnal.gov

March 14, 2015

We present the measurement of the diboson WW and WZ associate production in a final state consistent with semileptonic W decay plus heavy flavor quarks. This analysis uses the full dataset, collected with the CDF II detector at the Tevatron $p\bar{p}$ collider and corresponding to an integrated luminosity of approximately 9.4 fb^{-1}. Candidate signal events are required to have one charged lepton, kinematics consistent with the $W \to \ell\nu$ decay and two high E_T jets containing at least one secondary-decay vertex signaling the presence of heavy flavor hadrons. The analysis of the di-jet invariant mass spectrum allows to observe a 3.69σ evidence of the WW+WZ production in this final state and to extract a cross section measurement of $\sigma_{WW+WZ} = 13.7 \pm 3.9$ pb. The different heavy flavor decay pattern of the W and Z bosons (e.i. $W^+ \to c\bar{s}$, $Z \to b\bar{b}, c\bar{c}$) and the analysis of the secondary-decay vertex properties allow to independently measure the WW and WZ production cross section in a hadronic final state, for the first time at hadron colliders. The measured cross sections of $\sigma_{WW} = 9.4 \pm 4.2$ pb and $\sigma_{WZ} = 3.7^{+2.5}_{-2.2}$ pb are consistent with the SM predictions and correspond to a signal significances of 2.87σ and 2.12σ for WW and WZ respectively.

This note describes the search for the associate production of a W boson, decaying leptonically, and a W or Z boson, decaying hadronically in a Heavy-Flavor (HF) quark enriched final state. The difference in the vector bosons HF-decays, $W \to cs$ and $Z \to b\bar{b}/c\bar{c}$, is used for the separate measurement of the WW and WZ production modes.

The final state under investigation, containing exactly one lepton and HF-jets, is experimentally complex but of primary importance at hadron colliders.

For example, at the Tevatron $p\bar{p}$ collider, the most sensitive channel for the Standard Model (SM) Higgs boson search is the WH associate production where the Higgs decays to a b-quark pair and the W decays leptonically. The measurement of other SM resonances in the same final state is a confirmation of the validity of the Higgs boson searches and,

indeed, the first evidence for inclusive diboson production in the lepton plus HF-jet final state [1] was a milestone for the Higgs search at the Tevatron. Such analysis was based on a 7.5 fb^{-1} dataset and the signal was extracted by studying the di-jet invariant mass spectrum. Successively, by using the same advanced analysis techniques of the SM Higgs search, and a combination of the zero, one, and two lepton channel analyses, both the CDF and D0 collaborations [2] reported the evidence for WZ and ZZ combined production.

The measurement of the diboson cross section has also a first role in the landscape of SM physics as the different production modes (WW, WZ, ZZ) directly probe the triple and quadratic Gauge coupling terms of the SM. Diboson analysis in the purely leptonic decay channels has the advantages of a small amount of expected background and of the production modes separation according to the lepton multiplicity. This last feature is almost impossible to obtain with the analysis of semi-leptonic decay channels, where one of the two bosons decays hadronically, because of the small W/Z mass separation and of the low invariant-mass resolution. However, as described in the following, we achieved such goal by using the different W/Z HF decay pattern.

The analysis described in this paper uses the full dataset collected with the CDFII detector [5] at the Tevatron collider, corresponding to an integrated luminosity of approximately 9.4 fb^{-1} collisions at $\sqrt{s} = 1.96$ TeV. Candidate signal events are identified by one reconstructed light lepton (e or μ) and imbalance in the total transverse energy ($\not\!\!E_T$), signaling the $W \to \ell\nu$ decay. Successively, a Support Vector Machine (SVM) discriminant [6] is used to reject events inconsistent with $W \to \ell\nu$+jet production. Finally, the hadronic decay of the W or Z bosons is identified by requiring events with two high-p_T jets where, in at least one of them, a secondary-decay vertex indicates the presence of a b- or c-hadron (HF-tag). The resonant W or Z boson signal is extracted from the large non-resonant background by studying the di-jet invariant mass spectrum. In combination with this, a Flavor-separator [7] Neural-Network (Flavor-separator NN) is used to enhance the separation between $c-$ and $b-$jets, and therefore the sensibility to WW or WZ production modes. The strategy and the main features of this analysis are also described in details in [3], although the present result has superior sensitivity due to the introduction of improved analysis techniques.

1 Data Sample & Event Selection

We select events consistent with the signature of a W boson leptonic decay produced in association with two energetic HF jets. Selection starts online with an ensemble of different triggers that can be grouped in the following categories:

- central electrons: collected by requiring a track matched to a the central ($|\eta| < 1.1$) electromagnetic (EM) cluster with $E_T > 18$ GeV;

- central muons: collected by requiring a track with $p_T > 18$ GeV/c and matched a clear signal in one of the central ($|\eta| < 1.1$) muon chambers;

- forward electrons: collected by requiring an EM cluster in the forward calorimeter ($1.2 < |\eta| < 2.0$) and $\not\!\!E_T$ reconstructed online above 15 GeV;

- extended muons triggers: this group comprehend events selected by a combination of high energy jets and large $\not\!\!E_T$ requirements. The name of the category is due to the high fraction of $W \to \mu\nu$ events collected from these triggers: large online-reconstructed $\not\!\!E_T$ is often associated to the presence of both a neutrino and a muon because the muon momentum is not accounted in the online $\not\!\!E_T$ calculation.

The different trigger strategies sculpt the kinematic and the background composition of the selected data samples, therefore four main lepton analysis categories are defined according to them and used in the following.

At offline level we require exactly one charged lepton. Lepton candidates can be reconstructed by ten different identification algorithms which include: tight central electrons or muons with, five kind of loose muon identification criteria, forward electrons, and high p_T *isolated* tracks. All the leptons are required to be isolated from additional calorimetric activity, except for the latter track category where the isolation is required with respect to activity in the tracker. Electron (muon) candidates are required to have $E_T > 20$ GeV ($p_T > 20$ GeV/c). Successively we require two jets reconstructed with the `JETCLU` cone algorithm of radius $R = 0.4$ in the $|\eta_{Det}| < 2.0$ region and with $E_T^{corr} > 20$ GeV, after jet energy corrections for instrumental effects, and, when dealing with simulated events, for the quark or gluon origin of the jet. Finally we ask for $\not\!\!E_T > 15$ GeV, after correcting it for jet and muons in the event.

1.1 Suppression of Multi-jet Background

The use of loose lepton identification algorithms and low $\not\!\!E_T$ is well suited for the search of signals with small yield. However fake W-boson-like signatures, given by one jet faking the lepton identification and moderate $\not\!\!E_T$ from energy mis-measurement, are enhanced. We developed a method to suppress such, so-called, multi-jet background using multivariate discriminants built with the Support Vector Machine algorithm (SVM) [6]. Two discriminants, one for the central and one for the forward samples[1], have been trained to distinguish between simulated $W \to e\nu$+jets events and multi-jet events (obtained using a data-driven model). To deal with imperfections and biases in the signal or background models, a feedback from a data control sample is included in the training procedure.

[1]The multi-jet contamination is from two to three times higher in the forward reconstructed electrons with respect to the central electron selection.

The W+jet selection criteria is defined by a cut on SVM output distribution. Taking as example a threshold of SVM output greater than 0, the central SVM discriminant rejects about 90% of the multi-jet background with a signal efficiency above 93%. The forward SVM discriminant, using the same threshold, rejects about 75% of the background with similar signal efficiency.

Thanks to the good separation between the W+jets signal and the multi-jet background, the discriminating variables are used to fit the multi-jet background normalization, as shown in Figures 1, 2 and explained in Section 2.

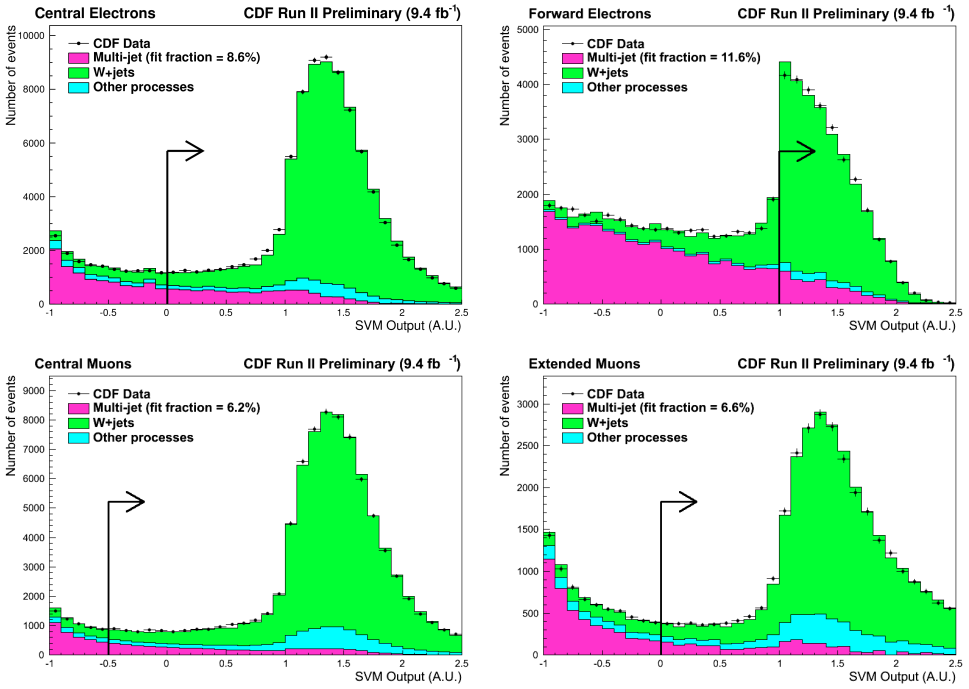

Figure 1: *W+jets (green) and multi-jet (pink) fraction estimates for the pretag control region derived from a fit on the SVM output distribution. The figure shows (left to right and top to bottom) central electrons, forward electrons, central muons, and extended muons lepton categories. The reported percentage refer to the fractions of the components beyond the signal selection cut pointed by the arrows.*

1.2 Definition of Signal and Control Regions

The selection criteria described until now, which does not distinguish between the flavor of the jets in the final state, it is named *pretag* selection. As we are looking for events

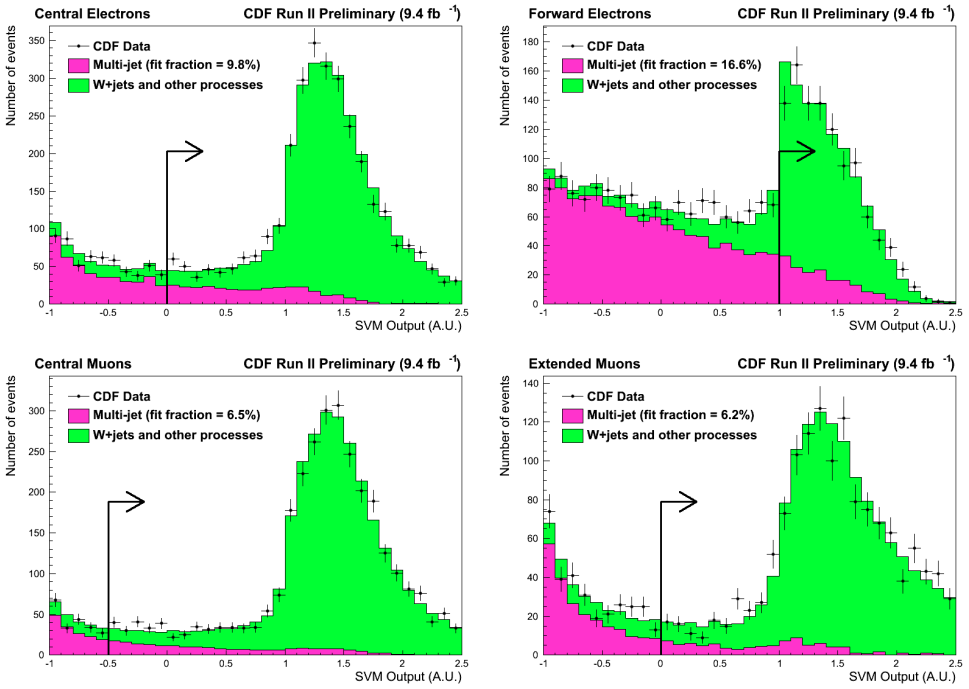

Figure 2: *Multi-jet (pink) fraction estimates for the 1-tag signal region derived from a fit on the SVM output distribution. The figure shows (left to right and top to bottom) central electrons, forward electrons, central muons, and extended muons lepton categories. The reported percentage refer to the fractions of the components beyond the signal selection cut pointed by the arrows.*

containing a W or Z bosons decay into heavy flavour, we further require that at least one of the two jets is containing a secondary decay vertex, *tagged* by the SecVtx algorithm [5] and signaling the presence of a HF-hadron in the jet. Thanks to this additional selection we classify the events in two signal enriched samples according to the presence of 1 or 2 tags.

The presence of a secondary-decay vertex allows to use two powerful algorithms exploiting additional properties of the jets and of the secondary-decay vertex itself. The already mentioned Flavor-separator NN assigns a score between -1 and 1 to each jet according if they are more b-like or LF-like, with jets originating from c-quarks likely to obtain negative scores clustering at -0.5. The b-jet energy calibration NN [8] which improves the b-jet energy resolution. Both these algorithms are used to improve the sensitivity to the signal.

2 Background Estimate

The selected events are likely to originate from $W \to \ell\nu$+HF final states. In addition to the signal, several other processes give such final state, therefore all the following backgrounds must be considered:

Multi-jet : a W-boson-like signature is generated when one jet fakes a high p_T lepton and $\not\!\!E_T$ is generated through energy mis-measurement.

W + Light Flavor: one or more Light Flavor (LF) jets is produced in association with a W boson and mistakenly identified as a HF-jet by the HF-tagging algorithm. Mistags are generated because of the finite resolution of the tracking detectors, material interactions, or from long-lived light flavor hadrons (Λ and K_s) which produce real displaced vertices. The mistag probability of a generic jet is measured in a multi-jet control sample and parametrized as a function of six significant variables ("mistag matrix").

W+ HF: these processes ($W + b\bar{b}$, $W + c\bar{c}$ and $W + c$) involve the production of a W boson in association with HF-quarks, mainly from radiated gluons. This represent the main irreducible background.

EWK: additional small background contributions come from single top quark and top quark pair production, Z boson + jets production, and, the almost negligible, WH and ZZ production. They have different origins therefore, when considered all together, they are simply labelled EWK.

The kinematic description of the W+jets (equal to the sum of $W + LF$ and $W + HF$) events is obtained by composing a large set of Alpgen+Pythia [9, 10] MC's weighted by their LO production cross section. We then determine the amount of selected W+jets events using a likelihood fit of the SVM distribution of the pretag data sample, separately in each lepton category. As shown in Fig. 1, two templates with free normalization are used for W+jets and multi-jet, while the EWK components are normalized to the theoretical expectations. The following data-driven models are used used to produce the multi-jet templates:

- for the electrons: inversion of 2 out 5 identification variables related to EM-shower shape and calorimeter cluster selection criteria;
- for the muons and the isolated tracks: inversion of isolation criteria applied to tight and loose muon selection algorithms.

The $\not\!\!E_T$ of the central electron multi-jet model is corrected to account for the different calorimeter response of the fake-electron in data and in the model with inverted selection.

The $HF-$tagged $W + HF$ background normalization is extracted from the total W+jets pretag sample. However the HF-fractions of $W + c$ and $W + b\bar{b}/c\bar{c}$ obtained

from the MC may a large correction (ex. due to NLO contributions) to match the data. We simultaneously derived $W+c$ and $W+b\bar{b}/c\bar{c}$ HF-fraction correction from the $W+1$jet control region as described in Appendix 4. The correction factor amounts to 1.24 with an uncertainty of 20% for $W+b\bar{b}/c\bar{c}$ and it is 1 ± 0.3 for $W+c$.

We estimate the normalization of $W+LF$ by applying the mistag matrix to the pretag data after subtracting the contribution from all the other backgrounds. We model the $W+LF$ HF-tagged kinematics using the $W+LF$ MC weighting each event for the mistag probability.

All the EWK backgrounds are normalized directly to their theoretical cross sections, calculated at next-to-leading order.

Finally the residual tagged Non-W component is fitted to the data together with a template of all the other backgrounds: the two normalizations are free to float and the multi-jet one is extracted.

More details on the background estimate can be found in Ref [11]. Table 1 summarizes the number of observed and expected events in the W+2 jets sample, for all lepton categories, for pretag, 1-tag, and 2-tags categories.

$W \to \ell\nu +$ 2jets		CDF Run II Preliminary (9.4 fb^{-1})	
Process	Pretag	1-tag	2-tag
multi-jet	20300 ± 2700	800 ± 330	30 ± 14
$W+LF$	161700 ± 3700	2440 ± 350	29.5 ± 6.8
$W+c\bar{c}$	13400 ± 1700	1190 ± 290	33 ± 10
$W+c$	11600 ± 2200	930 ± 310	12.5 ± 5.5
$W+b\bar{b}$	6370 ± 930	2190 ± 520	313 ± 81
Z+jets	9400 ± 1900	281 ± 42	13.5 ± 2.1
$t\bar{t}$	1600 ± 230	663 ± 94	137 ± 22
single-t	1109 ± 42	441 ± 23	70.8 ± 8.4
ZZ	93.4 ± 4.4	10.1 ± 0.7	2.0 ± 0.3
WH	40.0 ± 1.4	17.6 ± 0.8	5.4 ± 0.6
WW	5530 ± 400	240 ± 30	3.0 ± 0.7
WZ	904 ± 53	91.4 ± 7.6	17.2 ± 2.1
Total prediction	(fit to data)	9300 ± 1200	670 ± 110
Observed data	232145	9074	604

Table 1: Summary of observed and expected events in the pretag, 1-tag and 2-tag selection regions, in the W+2 jets sample, in 9.4 fb^{-1} of data.

3 Signal to Background Discrimination

We are searching for the decay of a resonance over a large background of non-resonant event, therefore the signal discrimination is based on the invariant mass of the two jets in the event: $M_{inv}(jet1, jet2)$. The jet energy is improved by the mentioned b-jet NN calibration thus decreasing the $M_{inv}(jet1, jet2)$ resolution. For 1-tag events, the Flavor-separator NN is used in combination with $M_{Inv}(jet1, jet2)$ to build a bi-dimensional distribution: the Flavor-separator NN output is divided in 7 bins such that the highest score ones are enriched in b-like secondary vertices, while the others have variable composition of b-like, c-like and mistag-like jets. As $W + b\bar{b}$ and $W + c/c\bar{c}$ have roughly the same yield, the result of the bi-dimensional classification is to divide by 2 the non-resonant background under the WW or WZ peaks respectively, without loss of any signal. The example of signal and two background templates is shown in Figure 3. Events with 2-tags are almost entirely generated by the $W + b\bar{b}$ and top backgrounds, with signal originating only from WZ production, therefore the $M_{inv}(jet1, jet2)$ distribution alone is used for the signal extraction.

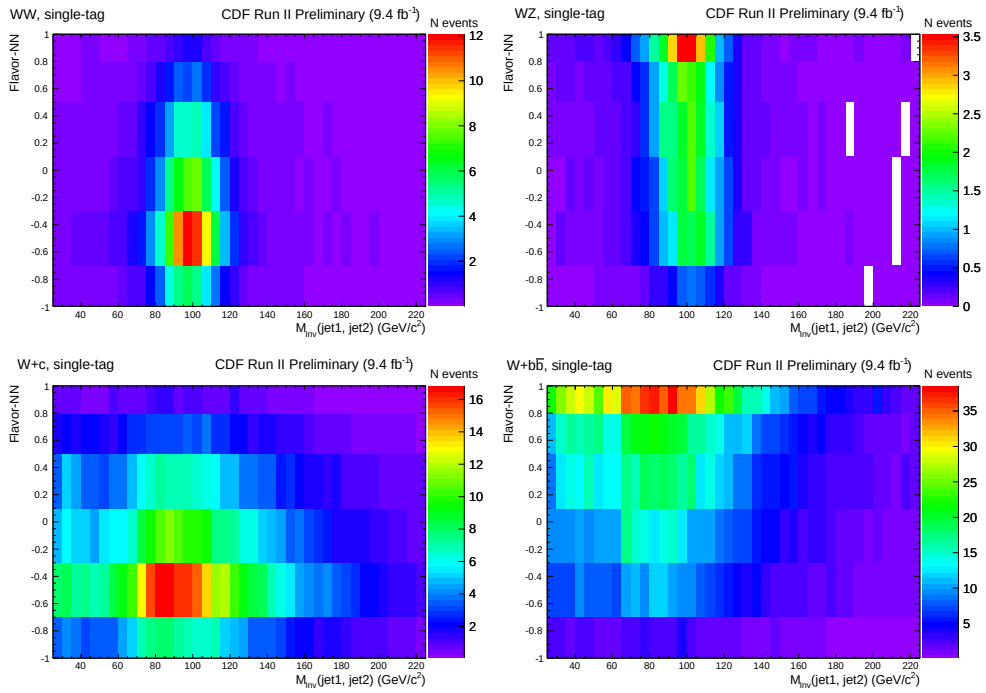

Figure 3: *Examples of $M_{Inv}(jet1, jet2)$ vs Flavor-separator NN templates used for 1-tag, W+2 jet events: for signal (WW on the top left, WZ on the top right) and two backgrounds ($W + c$ on the bottom left, $W + b\bar{b}$ on the bottom right).*

In total, eight different regions are used for the signal extraction: 4 lepton sub-samples (central electrons, central muons, forward electrons, extended muons) $\times$ 2 HF-tag prescriptions (1-tag with Flavor-separator NN and 2-tags). The distributions added for all the lepton category for the 1-tag channel are shown in Figure 4: on the left they are integrated across the Flavor-separator NN and projected on $M_{inv}(jet1, jet2)$, while on the integration is across $M_{inv}(jet1, jet2)$ and the projection is on the Flavor-separator distribution. Figure 5 shows the single-tag $M_{inv}(jet1, jet2)$ distribution when divided in the rightmost and b-enriched Flavor-separator NN region (Flavor-separator NN > 0.5) aside to the $M_{inv}(jet1, jet2)$ distribution resulting in the the lower score Flavor-separator NN bins (Flavor-separator NN < 0.5). Finally, the $M_{inv}(jet1, jet2)$ distribution for 2-tags events (added for all the lepton categories) is shown in Figure 6. The shown $M_{inv}(jet1, jet2)$ plots are obtained with a simultaneous fit of the signal and background normalizations, treating systematic uncertainties as nuisance parameters and taking into account correlated systematic effects (see next paragraph for a complete description).

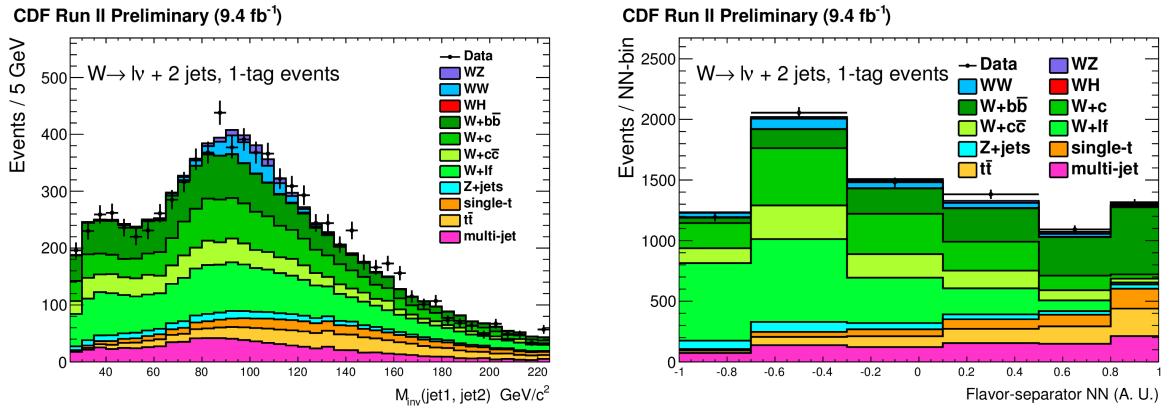

Figure 4: $M_{Inv}(jet1, jet2)$ *distribution for the 1-tag candidates where all the lepton category have been added together. The best fit of the systematic nuisance parameters are taken into account.*

3.1 Cross Section Measurement and Statistical Analysis

In order to measure the total and separate WW/WZ production cross sections in the HF-enriched final state, we compare the di-jet invariant mass spectrum of data to the expectation using a Bayesian statistical analysis.

A likelihood function is built using the observed bin-by-bin Poisson distribution of data, signal, and background estimates. The prior probabilities of background and signal templates are included in the likelihood, together with all rate and/or shape systematic

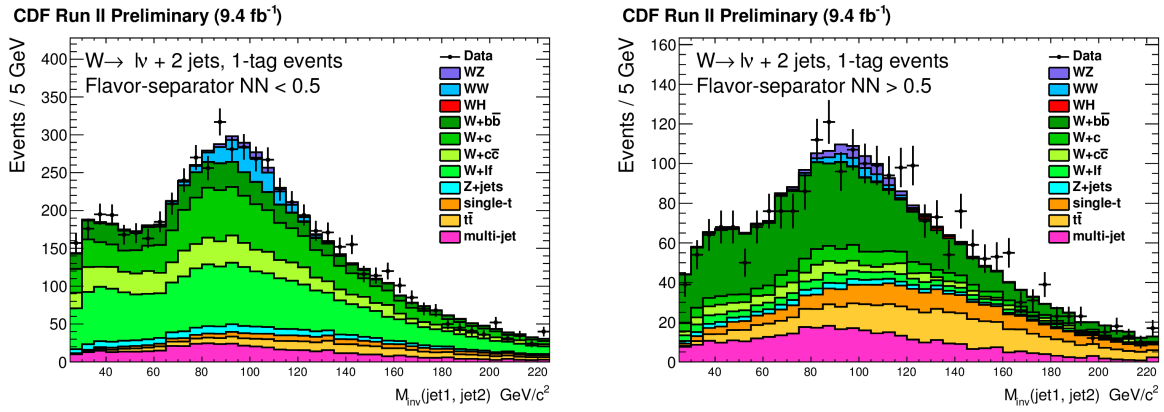

Figure 5: $M_{Inv}(jet1, jet2)$ *distribution for the 1-tag candidates, separate depending on the Flavor-separator NN score on the tagged jet: on left, in case with* $NN < 0.5$*, on the right the case with* $NN > 0.5$*. All the lepton category have been added together and the best fit of the systematic nuisance parameters are taken into account.*

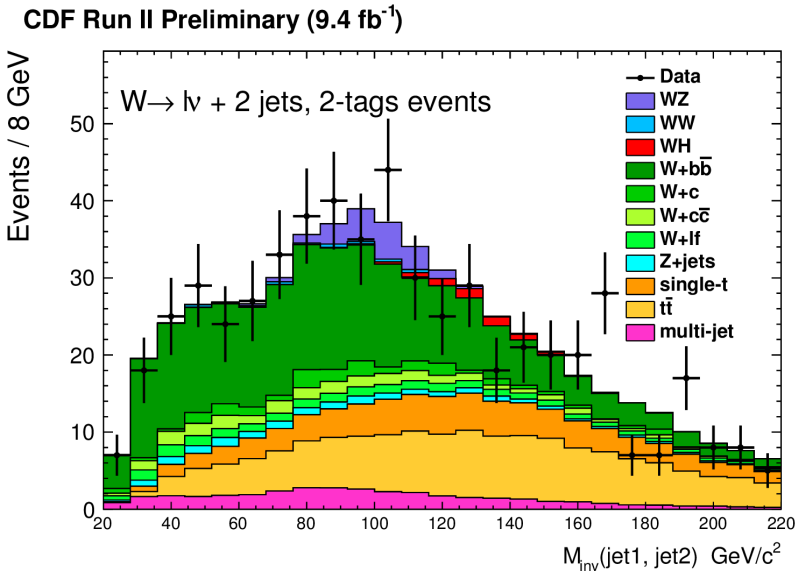

Figure 6: $M_{Inv}(jet1, jet2)$ *distribution for the 2-tag candidates where all the lepton category have been added together. The best fit of the systematic nuisance parameters are taken into account.*

uncertainties which are treated as nuisance parameters. The unknown yield of the two signal processes (WW and WZ) is parametrized by a uniform prior distribution bounded to be greater than 0. The signal measurement is obtained by integrating out the nuisance parameters and by studying the resulting Bayesian posterior distribution. As the initial signal parametrization is normalized to the SM expectation, the maximum value of the Bayesian posterior corresponds to the measurement of the signal strength μ:

$$\mu = (\sigma \times BR)^{obs}_{signal} / (\sigma \times BR)^{SM}_{signal} \quad (1)$$

The 68% coverage of the Bayesian posterior will provide the measurement uncertainty. In the cases where we evaluate the total $WW + WZ$ cross section, we will use a one-dimensional uniform signal prior and use the SM relative rates for the WW and WZ processes. When evaluating the separate WW and WZ cross sections, we use a two-dimensional uniform prior.

The following systematic uncertainties (for background and signal) are taken into account as normalization nuisance parameters (max-min variation is in parenthesis): JES (1–14%), Alpgen renormalization and factorization scale (1–17%), HF-tagging efficiency scale factors (SF) for b-quarks (3-11%), HF-tagging efficiency SF for c-quarks (8–22%), lepton identification and trigger efficiencies (1–4%), multi-jet background normalization (40%), Z+jet total normalization (40%), W+HF correction fractions (20–30%), ISR/FSR (1-4% for signal only) and mistag uncertainty (12–25%). In addition JES, Q^2, Flavor-separator NN c/light-flavor and multi-jet parametrizations, are taken as shape systematics as well, where the interpolated shape variation is used as nuisance parameter. All the nuisance parameters are integrated in the fit to improve the sensitivity.

The $WW + WZ$ signal cross section is first measured leaving the production cross section of the WW and WZ component constrained to the SM ratio. The resulting Bayesian posterior distribution is shown in Figure 7 together with the 68% and 95% confidence intervals, after scaling by $\sigma^{SM}_{WW} = 11.34$ plus $\sigma^{SM}_{WZ} = 3.47$ pb. We obtain a cross section of:

$$\sigma^{Obs}_{WW+WZ} = 13.7 \pm 3.9 \text{ pb}. \quad (2)$$

To compute the significance of the measurement we performed a hypothesis test comparing data to the Null hypotheses (H_0): H_0 assumes all the predicted background processes except WW+WZ production. Pseudo-experiments (PEs) extracted from H_0 distribution. Figure 8 shows the possible outcomes of many cross section measurements in a background-only and in a background+signal hypothesis. The number of times a background fluctuation produces signal strenght measurement of $\mu^{Obs}_{WW+WZ} = 0.92$ gives a $p-$value of 0.00022. The results is an evidence for the WW+WZ production in $\ell\nu + HF$ final state with a significance of 3.69σ.

On a successive step we separately measure the WW and WZ processes. We iterated the cross section measurement procedure but, this time, σ_{WW} and σ_{WZ} are left free to

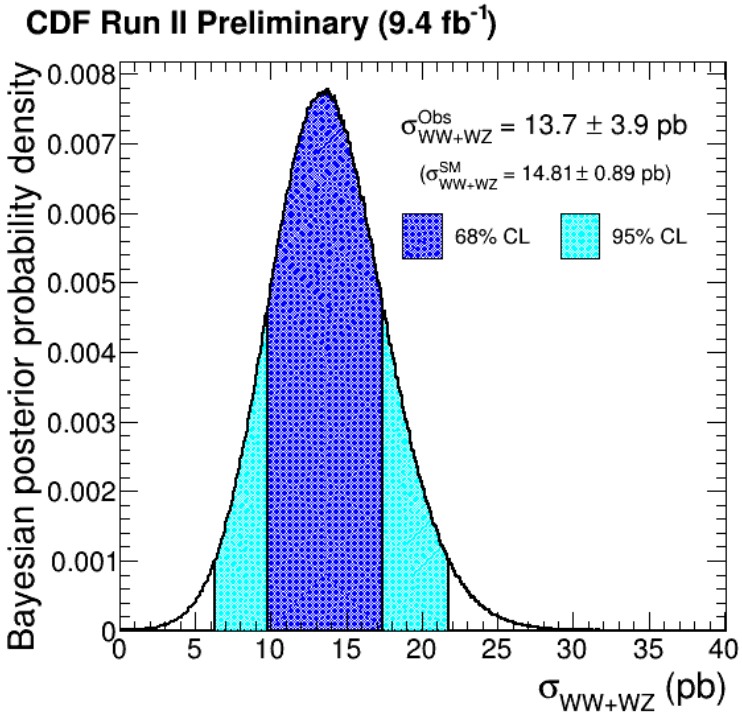

Figure 7: *Bayesian posterior distribution after marginalization over the nuisance parameters. The maximum value is the measured cross-section value. The blue and azure areas represent the smallest intervals enclosing 68% and 95%, of the posterior integrals, respectively.*

float independently (i.e. not constrained to the SM ratio). Figure 9 shows the measured Bayesian posterior distribution scaled to SM expectation, with integration contours at 1, and 2 σ confidence levels. The maximum value corresponds to measured cross section of $\sigma_{WW}^{Obs,2D} = 9.4$ pb and $\sigma_{WZ}^{Obs,2D} = 3.7$ pb, and signal strengths of $\mu_{WW}^{Obs,2D} = 0.83$ and $\mu_{WZ}^{Obs,2D} = 1.07$.

To analyze WW and WZ channels separately, we projected the two-dimensional Bayesian posterior on the σ_{WW} and the σ_{WZ} axes, in this way we consider, one at the time, the two processes as background. For both WW and WZ we re-computed maximum values and confidence intervals, results are shown in Figures 10. The measured cross sections values are identical but we have an immediate interpretation of the uncertainties:

$$\sigma_{WW}^{Obs} = 9.4 \pm 4.2 \text{ pb}, \tag{3}$$

$$\sigma_{WZ}^{Obs} = 3.7^{+2.5}_{-2.2} \text{ pb}. \tag{4}$$

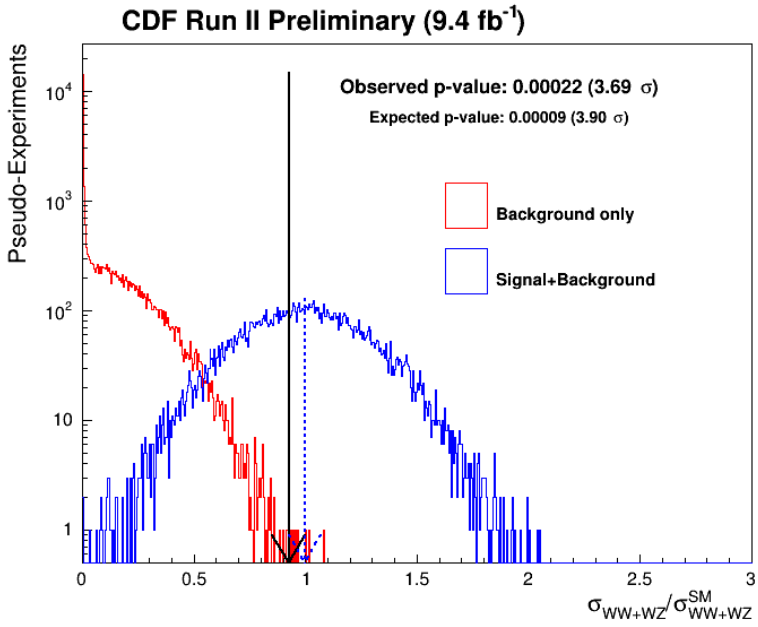

Figure 8: *Possible outcomes of many WW+WZ cross section measurements on Pseudo Experiments (PEs) generated in a background-only and in a background+signal hypothesis. The* $p-value$ *for* $\mu^{Obs}_{WW+WZ} = 0.92$ *is* 0.00022*, corresponding to a significance of* 3.69σ*.*

WW and WZ significances have been evaluated in a similar way: we generated PEs with *null hypothesis* on both WW and WZ signals. Then, the cross sections measured on the σ_{WW} vs σ_{WZ} plane have been projected along the axes and compared with σ^{Obs}_{WZ} and σ^{Obs}_{WZ}. The result of the $p-$value estimates are reported in Figure 11, we obtain: p-value$_{WW} = 0.00405$ and p-value$_{WZ} = 0.03388$. They correspond to a significance of 2.87σ and 2.12σ for WW and WZ respectively.

4 Conclusions

We analyzed the full CDFII dataset, corresponding to 9.4 fb^{-1} of data, looking for the $WW + WZ \rightarrow \ell\nu + HF$ signal in the $W + 2$ jets exclusive sample. Analyzing the $M_{inv}(jet1, jet2)$ spectrum and looking at the double and single HF-tagged events we measure a cross section of $\sigma_{WW+WZ} = 13.7 \pm 3.9$ pb with an uncertainty of less than 30%. The result is consistent with an evidence (3.69σ) for WW+WZ associate production and with the SM expectations.

Using different HF-decay pattern of the W and Z bosons ($W \rightarrow cs$ and $Z \rightarrow c\bar{c}, b\bar{b}$) we

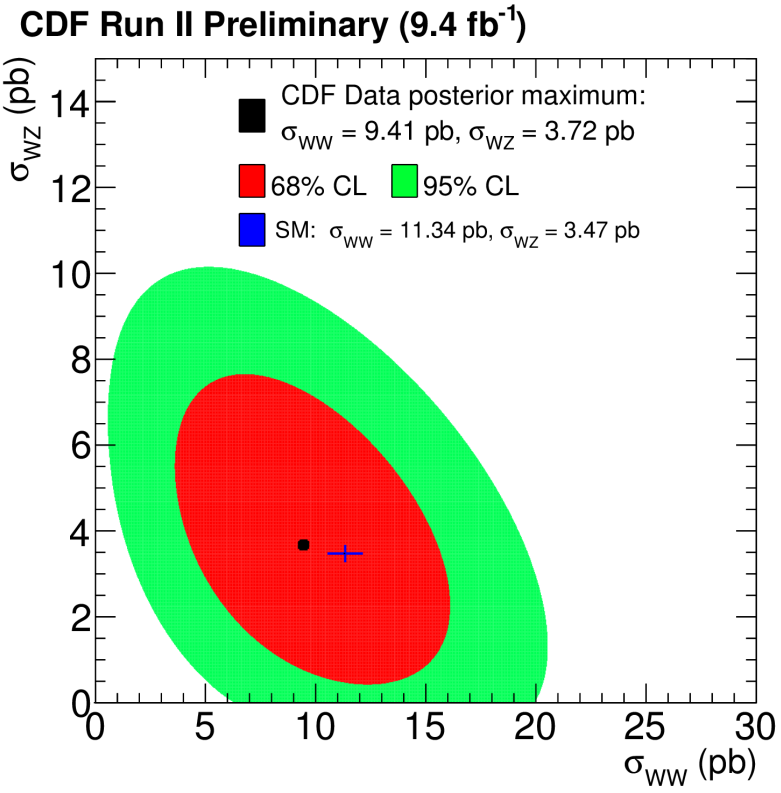

Figure 9: *The Bayesian posterior, marginalized over nuisance parameters and scaled to SM expectation, is shown in the plane σ_{WW} vs σ_{WZ}. The measured cross sections correspond to the maximum value of $\sigma_{WW}^{Obs,2D} = 9.4$ pb and $\sigma_{WZ}^{Obs,2D} = 3.7$ pb. The red and green areas represent the smallest intervals enclosing 68% and 95% of the posterior integrals, respectively.*

could measure separately the WW and WZ processes. We obtained $\sigma_{WW} = 9.4 \pm 4.2$ pb and $\sigma_{WZ} = 3.7^{+2.5}_{-2.2}$ pb, measuring for the first time the two processes independently in an hadronic final state. The observed significances of 2.87σ and 2.12σ for WW and WZ respectively, is consistent with the SM predictions.

Acknowledgments

We thank the Fermilab staff and the technical staffs of the participating institutions for their vital contributions. This work was supported by the U.S. Department of Energy and National Science Foundation; the Italian Istituto Nazionale di Fisica Nucleare; the

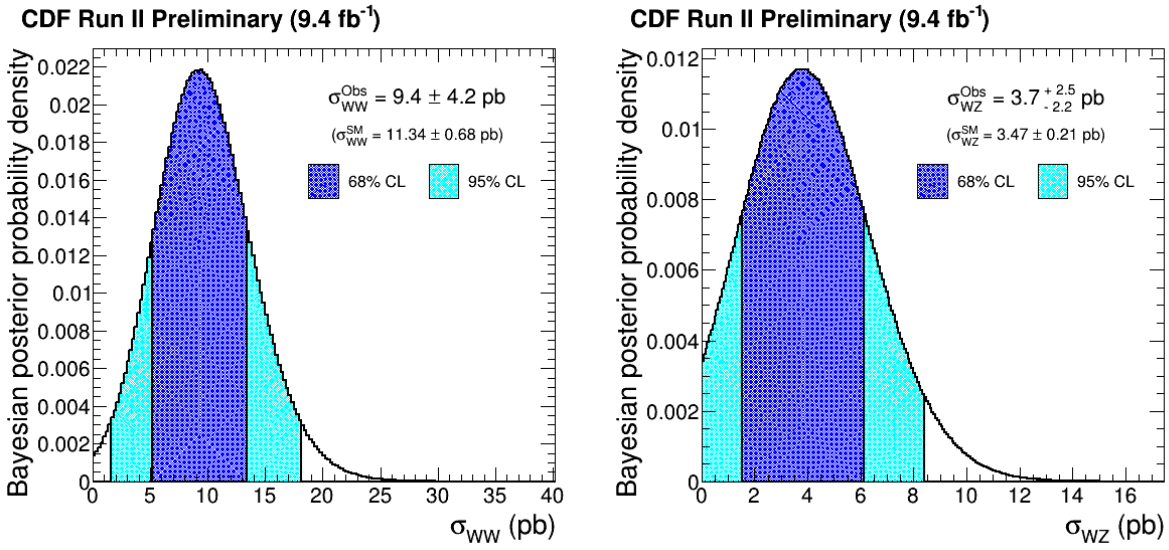

Figure 10: *The Bayesian posterior, function of σ_{WW} and σ_{WZ} marginalized over nuisance parameters, is shown after projection on the σ_{WW} (left) and σ_{WZ} (right) axes. The measured cross sections correspond to the maximum value the projected posterior: $\sigma_{WW}^{Obs} = 9.4 \pm 4.2$ pb and $\sigma_{WZ}^{Obs} = 3.7^{+2.5}_{-2.2}$ pb. The blue and azure areas represent the smallest intervals enclosing 68% and 95% of posterior integrals, respectively.*

Ministry of Education, Culture, Sports, Science and Technology of Japan; the Natural Sciences and Engineering Research Council of Canada; the National Science Council of the Republic of China; the Swiss National Science Foundation; the A.P. Sloan Foundation; the Bundesministerium fuer Bildung und Forschung, Germany; the Korean Science and Engineering Foundation and the Korean Research Foundation; the Particle Physics and Astronomy Research Council and the Royal Society, UK; the Russian Foundation for Basic Research; the Comision Interministerial de Ciencia y Tecnologia, Spain; and in part by the European Community's Human Potential Programme under contract HPRN-CT-20002, the Slovak R and D agency and the Academy of Finland.

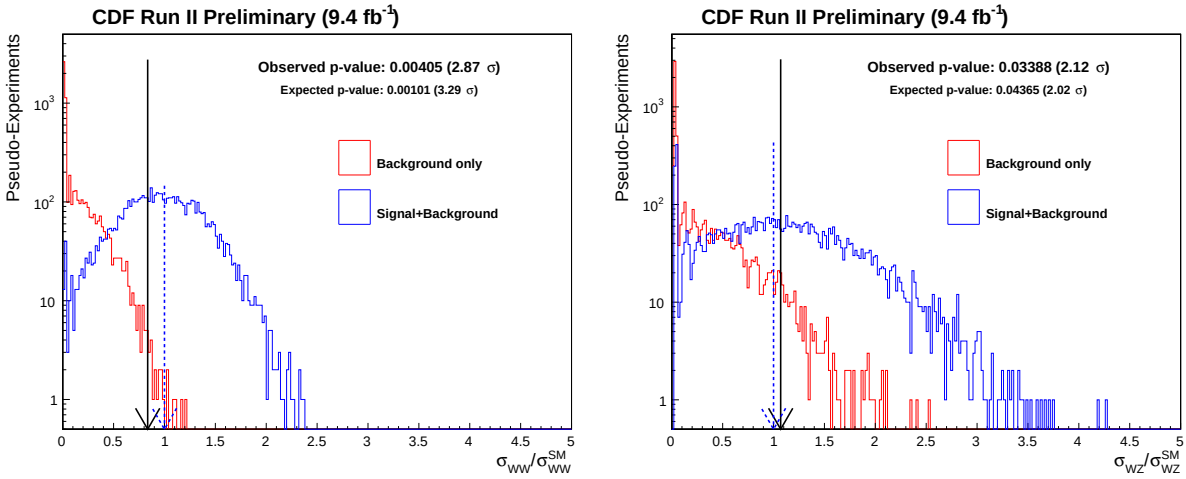

Figure 11: *Possible outcomes of many WW+WZ cross section measurements on Pseudo Experiments (PEs) generated in a background-only and in a background+signal hypothesis in the σ_{WW} vs σ_{WZ} plane and then projected on the σ_{WW} (left) and σ_{WZ} (axis). The p-values of* 0.00405 *and* 0.03388 *correspond to a significance of* 2.87σ *and* 2.12σ *for WW and WZ respectively.*

Appendix: Extraction of W+HF Correction Factor

The HF normalization factor used to correct the $W + HF$ background estimate should be derived from data. In this analysis we use the $W + 1$jet region for simultaneous derivation of the $W + b\bar{b}/c\bar{c}$ and $W + c$ correction factors. In practice a new analysis is performed, as described in the main text, with the following differences:

- only the tight central lepton identification algorithms and triggers are used for the $W \to \ell\nu$ candidates selection, thus giving two lepton categories.
- Exactly one tight jet is required in the event: the 1-jet pretag control region and 1-tag signal regions are therefore identified. The result of the W+jet and multi-jet normalization fits in the pretag regions are reported in Fig. 12.

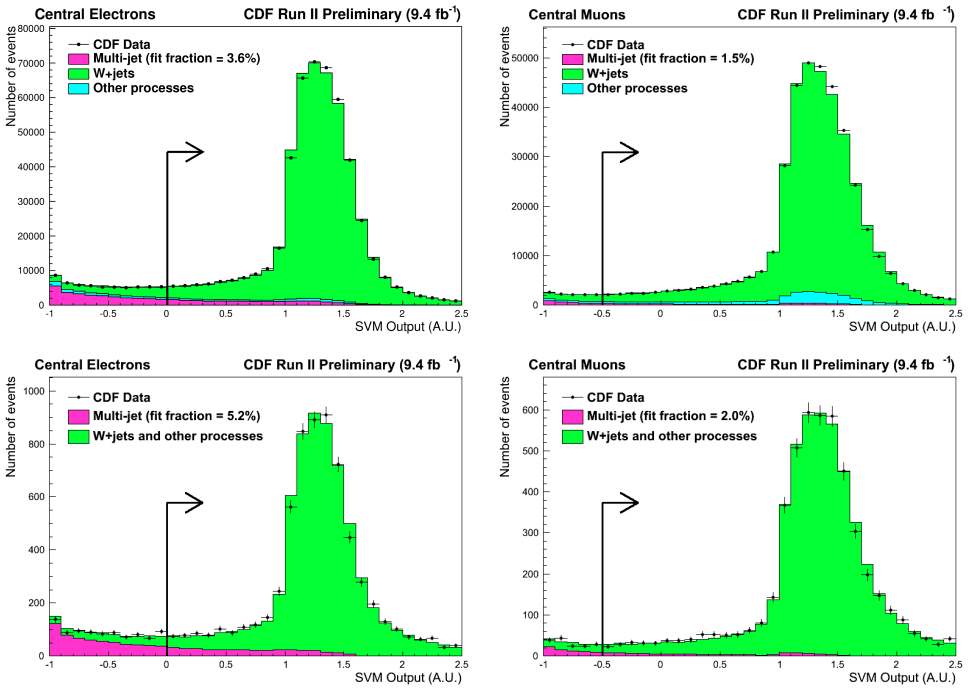

Figure 12: Multi-jet fraction estimate based on the fit of the SVM distributions. Pretag, one jet samples: central electrons (top left), central muons (top right). Single-tag, one jet samples, central electrons (bottom left), central muons (bottom right); The multi-jet background is shown in pink.

- Two signals are investigated, $W+b\bar{b}$ plus $W+c\bar{c}$, and $W+c$, with their discrimination based on the Flavor-separator NN distribution (shown in Fig. 13). The analysing

of a 2-dimensional Bayesian posterior distribution returns the signal-strength of the two processes. The signal strength is the ratio between the input HF correction factor and the one favored by the data.

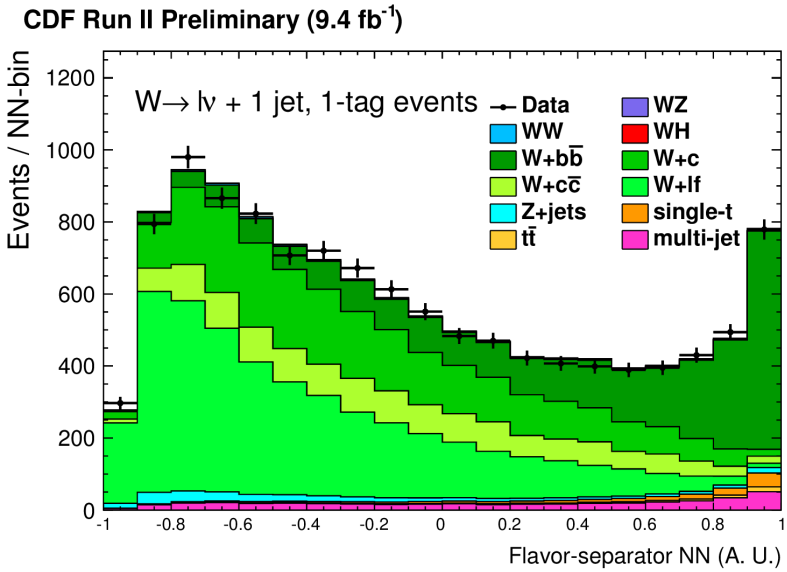

Figure 13: Flavor-separator NN distribution for the W plus one tagged jet, central muons and electrons. Systematic uncertainties are fit to data.

The analysis procedure has been iterated 4 times showing, in the last iteration, stable HF correction factors. The result of the last iteration is shown in Figure 14: $K_{cc} = K_{bb} = 1.24$, with 20% uncertainty, $K_c = 1.0$, with 30% uncertainy. The simultaneous extraction of K_c vs $K_{bb/cc}$ has been performed for the first time.

References

[1] G. Chiarelli, S. Leone, F. Sforza, "Search for $WW/WZ \to \ell\nu + HF$ jets vector boson production in 7.5 fb-1 of CDF data", CDF Public Note 10703 (2011); F. Sforza, *Evidence for* $WZ/WW \to l\nu + HeavyFlavors$ *Vector Boson Production in* 7.5 fb^{-1} *of CDF Data*, Proceedings of the DPF-2011 Conference (Oct 2011). arXiv:1110.0143v1.

[2] T. Aaltonen *et al.*, "Evidence for a Particle Produced in Association with Weak Bosons and Decaying to a Bottom-Antibottom Quark Pair in Higgs Boson Searches at the Tevatron", Phys. Rev. Lett. 109, 071804;

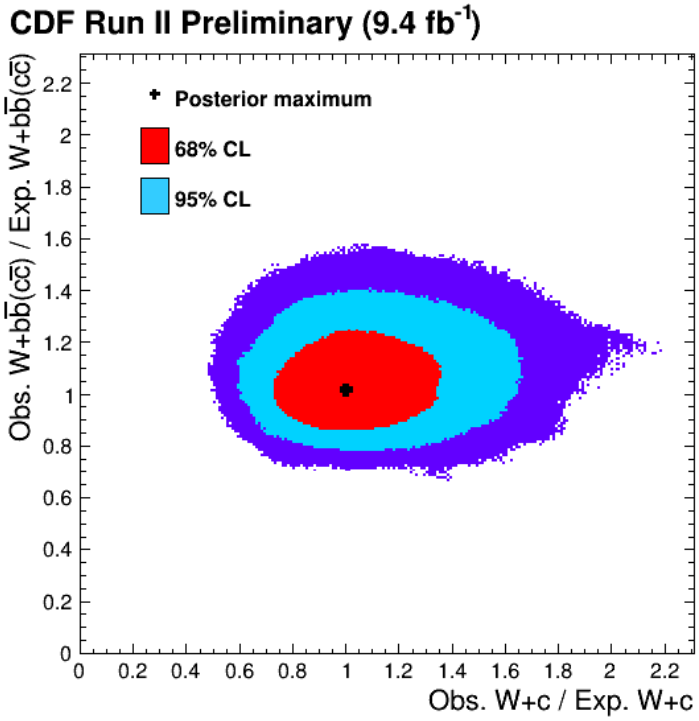

Figure 14: 2-Dim Bayesian posterior of $W + b\bar{b}$ plus $W + c\bar{c}$ versus $W + c$ signal strengths. The signal strength is the ratio between the input HF correction factors (used during the background estimate) and the one favored by the data.

[3] F. Sforza, "Evidence for Diboson Production in the Lepton plus Heavy Flavor Jets Final State at CDF", FERMILAB-THESIS-2012-41, 2012, arXiv:1302.0389 [hep-ex].

[4] F. Abe et al."Topology of three-jet events in $p\bar{p}$ collisions at $\sqrt{s} = 1.8$ TeV", Phys. Rev. D **45** (1992).

[5] D. Acosta, et al., Phys. Rev. D **71**, 052003 (2005).

[6] F. Sforza and V. Lippi, *Support vector machine classification on a biased training set: multi-jet background rejection at hadron colliders*, Nucl. Inst. and Meth. A, 722 (2013), arXiv:1407.0317.

[7] S. Richter *et al.*, "A Neural Network b Tagger for Single-Top Analysis", CDF Internal Note 7816. 2006; T. Chwalek *et al.*, "Update of the neural network b tagger for single-top analysis", CDF Internal Note 8903, 2008.

[8] T. Aaltonen, Y. Nagai, B. Kilminster, W. Yao, "Improved b-jet Energy Correction for $H \to b\bar{b}$ Searches at CDF", arXiv:1107.3026 [hep-ex], 2011.

[9] M.L. Mangano et al, JHEP 0307:001,2003, hep-ph/0206293.

[10] T Sjostrand et al., T. Sjostrand et al., High-Energy-Physics Event Generation with PYTHIA 6.1, Comput. Phys. Commun. **135**, 238 (2001).

[11] T. Aaltonen et al. (CDF Collaboration), Phys. Rev. D **82**, 112005 (2010).

Kinematic Distributions of Signal and Control Regions

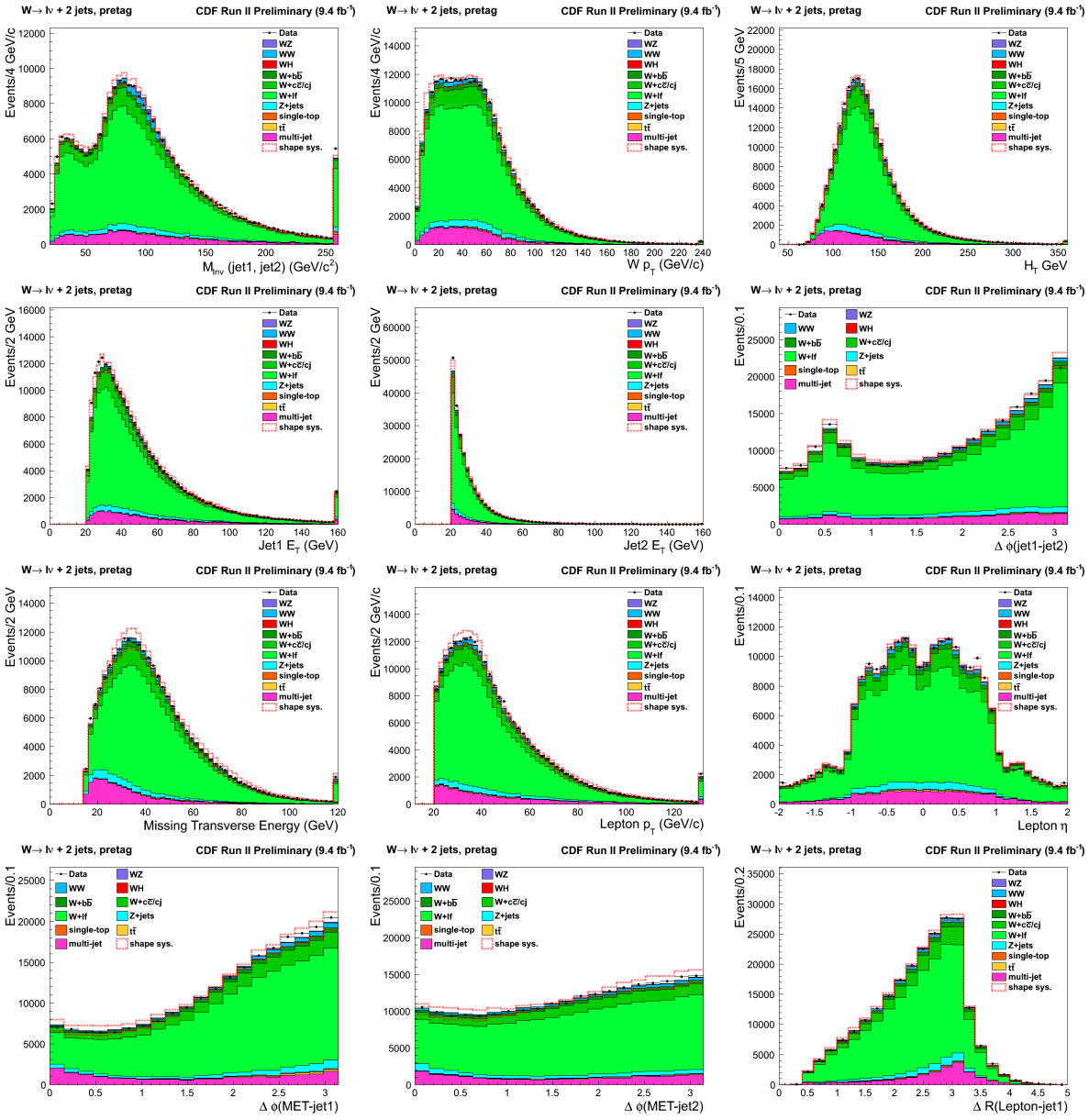

Figure 15: Kinematic distribution of the W + 2jets, pretag, control region. Signal and background normalizations are extracted from the discriminating variables fit, shape uncertainties are added in quadrature in each bin and overlaid as a dashed red line.

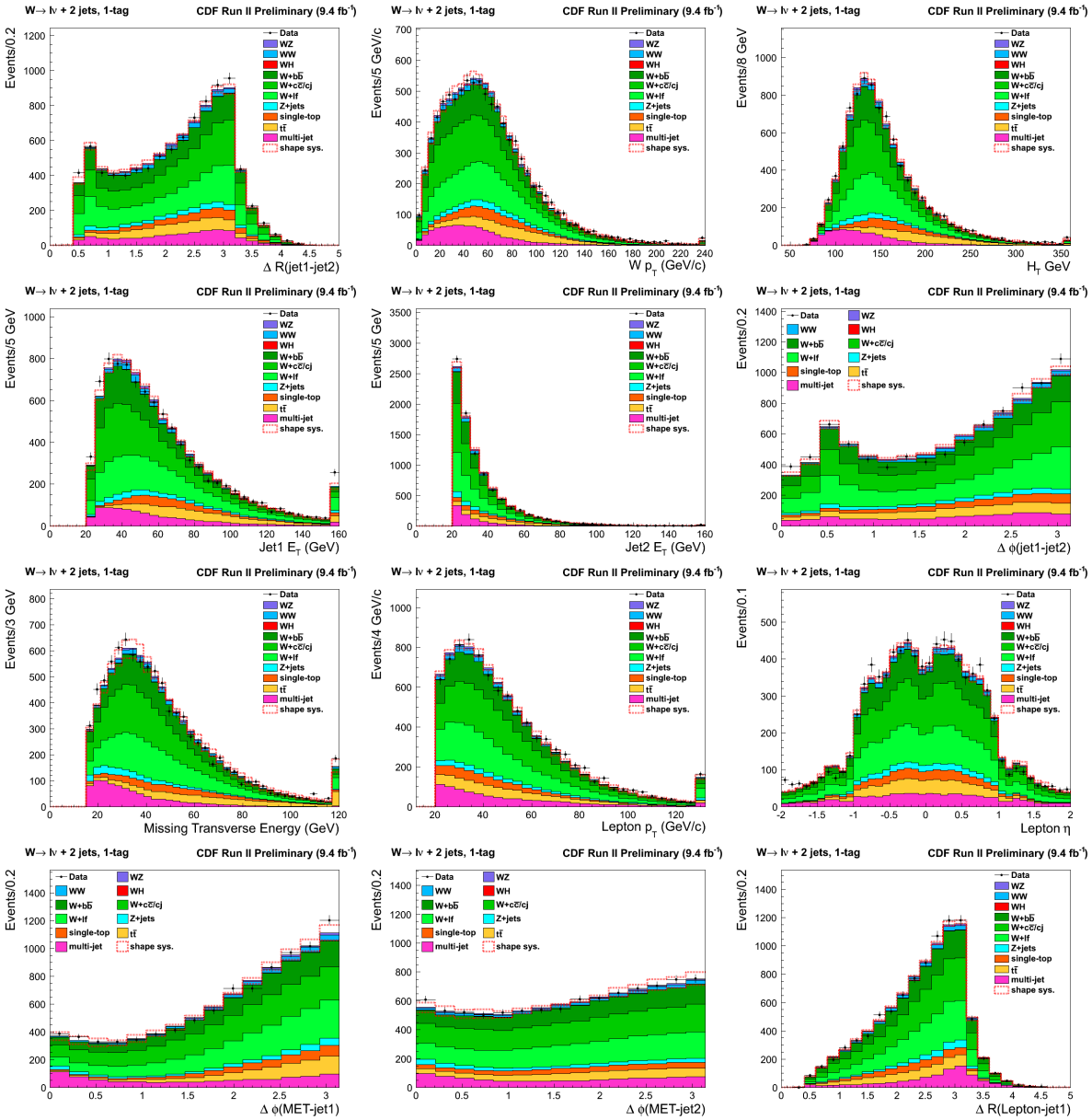

Figure 16: Kinematic distribution of the W + 2jets, 1-tag, signal region. Signal and background normalizations are extracted from the discriminating variables fit, shape uncertainties are added in quadrature in each bin and overlaid as a dashed red line.

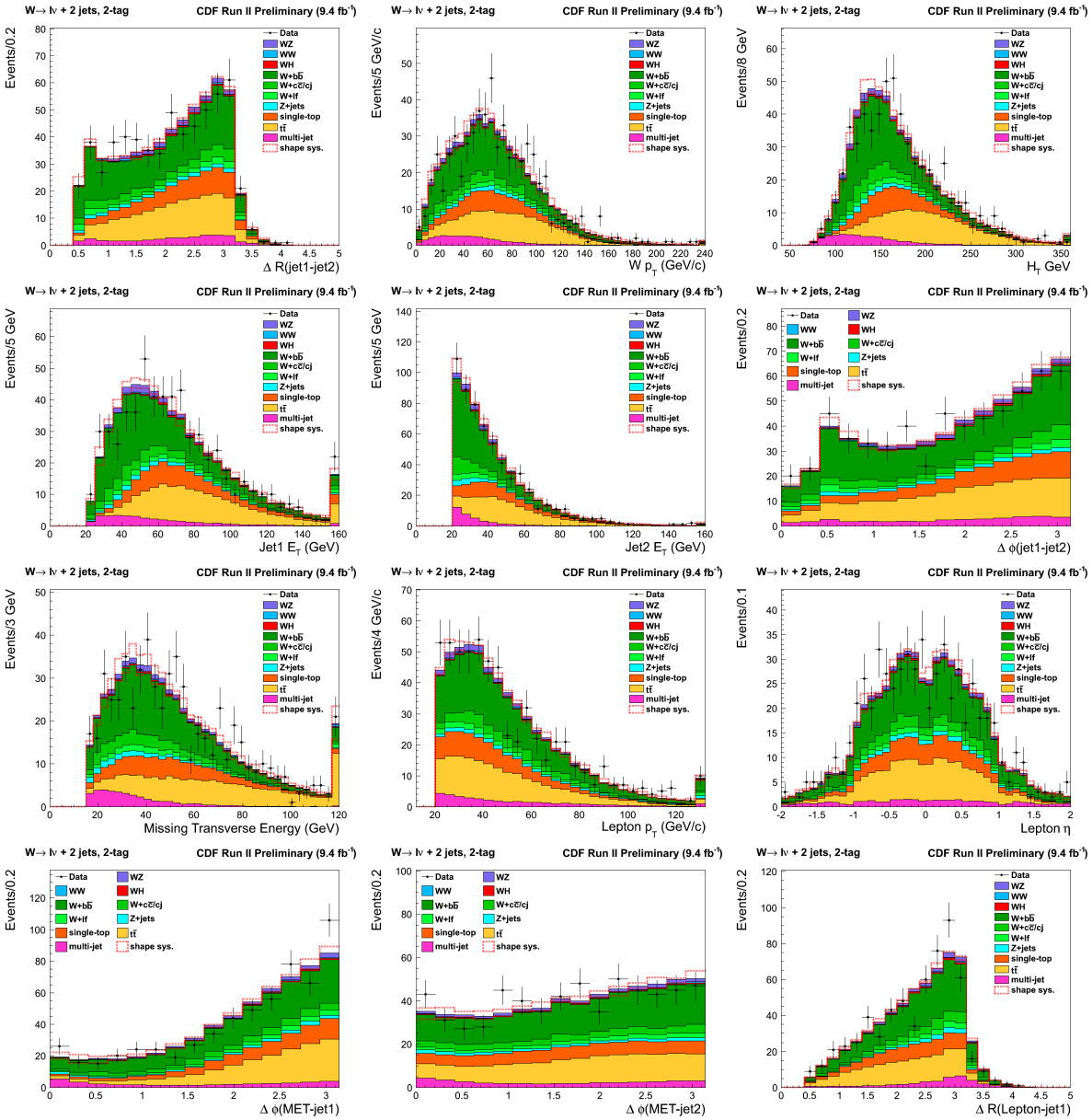

Figure 17: Kinematic distribution of the W + 2jets, 2-tag, signal region. Signal and background normalizations are extracted from the discriminating variables fit, shape uncertainties are added in quadrature in each bin and overlaid as a dashed red line.

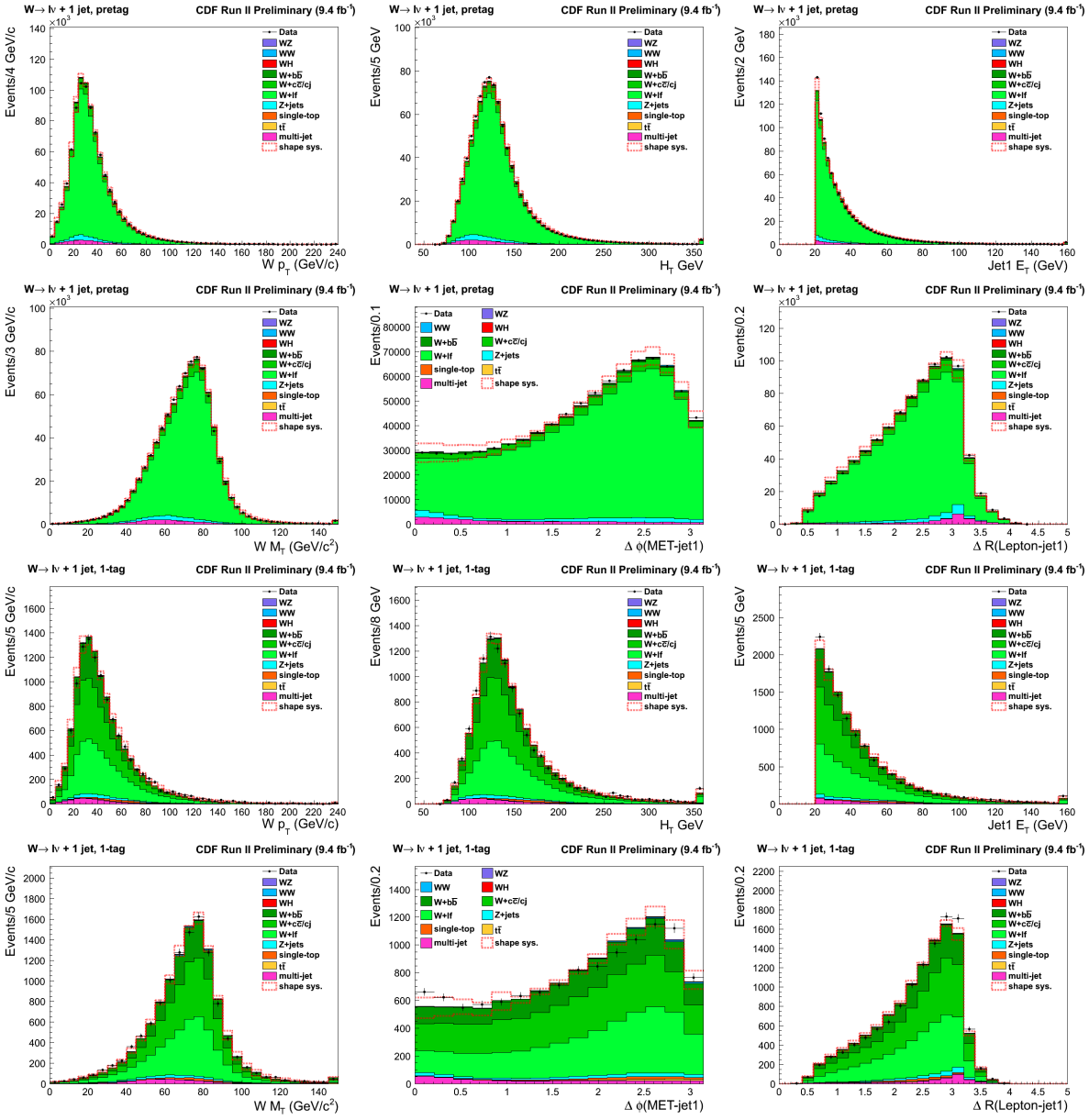

Figure 18: Kinematic distribution of the W + 1jet, control region: the top six distributions refer to the pretag control region, while the bottom six distributions refer to the 1-tag region used for the W+HF correction factor. Signal and background normalizations are extracted from the discriminating variables fit, shape uncertainties are added in quadrature in each bin and overlaid as a dashed red line.